Catalysis Today 390-391 (2022) 272–280

Contents lists available at ScienceDirect

Catalysis Today

journal homepage: www.elsevier.com/locate/cattod

Catalytic activity enhancement in pillared zeolites produced from exfoliated MWW monolayers in solution

Karolina Ogorzały [a], Gabriela Jajko [a], Karol Wolski [a], Szczepan Zapotoczny [a], Martin Kubů [b], Wieslaw J. Roth [a], Barbara Gil [a,1,*], Wacław Makowski [a,2,*]

[a] Jagiellonian University, Faculty of Chemistry, Gronostajowa 2, 30-387 Kraków, Poland
[b] Department of Physical and Macromolecular Chemistry, Faculty of Science, Charles University, Hlavova 8, 12840 Prague 2, Czech Republic

ARTICLE INFO

Keywords:
Layered zeolites
MCM-56
Alcohol-assisted pillaring
Catalysis
Friedel-Crafts alkylation

ABSTRACT

Layered zeolites, especially MWW, have been used to synthesize pillared micro/mesoporous hybrids with the goal to enhance catalytic activity towards larger molecules. The critical preparation step is expansion of the interlayer space by swelling with cationic surfactants at high pH. Recently reported solutions of MWW monolayers, obtained by exfoliation of the zeolite MCM-56, can be used to prepare analogous materials by flocculation (precipitation) with surfactant solutions. This previously unavailable approach is studied in this work with both high pH (0.2 M, pH > 13.3) and lower pH (0.01 M, pH~12) solutions, and resulted in finding conditions for preparation of catalysts that can be more active than pure microporous layers (zeolite) despite large content of unreactive silica pillars. Both the high and low pH conditions afforded similar expanded surfactant-MWW composites, but their behavior differed during pillaring with TEOS. Well-defined expanded interlayer distances indicated by a low angle reflection in XRD above 3 nm d-spacing was observed only with the high alkalinity preparations. An additional benefit was observed with TEOS treatment in the presence of isopropyl alcohol leading to a product showing high catalytic activity in model alkylation reaction (mesitylene with benzyl alcohol) proceeding faster than with the pure zeolite. The products obtained under different conditions were characterized by textural methods, nitrogen adsorption and QE-TPDA, and FT-IR to investigate acid site parameters. Notably, the MCM-56 used in this work was prepared with addition of aniline as the structure-promoting agent and is the second formulation affording exfoliable MWW materials.

1. Introduction

Zeolites are one of the major classes of heterogeneous catalysts with diverse microporous structures combined with high activity, shape selectivity, thermal resistance and potential for modification [1]. They play an important role in petroleum industry in various commercial processes including hydrocracking, isomerization and aromatization [2–4]. Zeolites are prominent in green chemistry, especially in replacement of environmentally problematic processes with cleaner technologies [5].

The field of conventional zeolites with rigid 3-dimensional structures, exemplified by the 'big five' – FAU, MFI, MOR, FER, BEA as well as others [6,7], has become quite mature from the point of view of practical applications. The discovery of layered zeolite precursors and other 2-dimensional (2D) forms has offered many new possibilities adding the potential of post-synthesis expansion and modification by design [8,9]. The initial efforts focused on swelling the MCM-22P precursor with cationic surfactants and subsequent pillaring with tetraethyl orthosilicate (TEOS) resulting in the material designated MCM-36 [10] and delamination by ultrasonication producing ITQ-2 [11]. Diverse modification methods provided new tools to explore improvement and expansion of existing applications by preparation of more active or efficient catalyst based on increased access to active sites and more open architectures [12,13]. Layered zeolites have been especially studied towards catalytic conversion of larger molecules because of constrains imposed by the 3D frameworks [14,15].

The investigation of 2D zeolites indicated potential for significant, practical benefits due to flexible structures that might allow better

* Corresponding authors.
E-mail addresses: barbara.k.gil@uj.edu.pl (B. Gil), waclaw.makowski@uj.edu.pl (W. Makowski).
[1] ORCID ID: 0000-0003-4096-0762
[2] ORCID ID: 0000-0002-4055-9664

https://doi.org/10.1016/j.cattod.2021.10.004
Received 29 June 2021; Received in revised form 24 August 2021; Accepted 6 October 2021
Available online 12 October 2021

exploitation of their catalytic activity and generation of more complex hierarchical structures [16]. By analogy to other 2D solids [8], zeolites have been subjected to modification methods [12,17] such as swelling and pillaring [10,18], delamination [11,16,19], but also provided unprecedented forms, e.g. interlamellar expanded zeolites as ordered pillared materials [20]. All this has been done with the goal of production of materials with higher catalytic activity, where mass transport of molecules can be facilitated.

Commercially used zeolite MWW with medium pores and large surface cavities [21] showed particular facility for producing 2D forms, directly or post-synthesis [13,22]. Its high Al form, MCM-56, can be considered a delaminated zeolite, comprising disordered stacks of layers without connection (in the ideal), that is obtained by direct synthesis [23,24]. It is so far the only directly synthesized delaminated zeolite among the 20 odd zeolites with confirmed 2D structures (all frameworks should be capable to make layers). The delaminated nature of MCM-56 has been confirmed by the recently reported achievement of direct, spontaneous exfoliation into monolayers in the liquid phase upon treatment with solutions of tetrabutylammonium hydroxide (TBAOH) [25]. This is a high yield treatment, e.g. 70% w/w layers vs. the starting MCM-56 solid, with few technical obstacles to being scaled-up, if justified. In contrast to the direct exfoliation used herein, the prior approaches, like delamination, required surfactant swelling and multi-step processing affording very low yield of monolayers in solution [16]. The key to the high yield direct exfoliation are suitable synthesis mixture compositions and conditions for preparation of the initial zeolite material, which presumably must be obtained with low level of layer/-crystal intergrowths. This aspect is still in the trial-and-error stage for other frameworks. An especially interesting approach to the synthesis of MCM-56 and others has been utilization of aniline as a structure-promoting agent [26] in addition to hexamethyleneimine (HMI) as the structure directing agent. This method, named temperature-controlled phase transfer hydrothermal synthesis, allowed reduced usage of the HMI exhibiting high toxicity, but seemed to be even more beneficial in another respect – MCM-56, which so far has been formed only as an intermediate converting to the 3D MCM-49 upon prolonged synthesis, was found to be effectively the end product. This has significant implications for its larger scale synthesis and the product has one of the highest acid activities among reported MCM-56 preparations. Its additional unexpected quality was facile exfoliation into monolayers in solution, which was exploited in this work.

Zeolite monolayers dispersed in a solution are like gigantic molecules that provide virtually unlimited potential for preparation of derivative structures and composites with other active components by reassembly and flocculation as solids [13,27,28]. This potential is investigated herein for the preparation of pillared derivatives including by an effective approach developed in our group [29], based on the original idea of Letaïef et al. [30], in which alcohols were used as a medium controlling hydrolysis of TEOS in pillaring of clay minerals. It was shown that the addition of alcohol during the pillaring process can lead to high overall catalytic activity, despite apparent reduction of acid site concentration caused by the introduction of inert silica and potential degradation during treatments.

The aim of this work was:

1) to study the exfoliation of MCM-56 zeolite synthesized in the presence of aniline,
2) to examine the effect of alkalinity of the exfoliated MWW monolayer solutions on the properties of eventual pillared samples,
3) to compare two pillaring methods based on catalytic activity of the pillared MWW catalysts.

The preparation procedures consisted of reacting the solutions of exfoliated MWW layers with the cationic surfactant cetyltrimethylammonium chloride (CTMACl), which afforded composites equivalent to swollen MWW precursors, pillaring with TEOS using different conditions and calcination.

2. Experimental

2.1. Preparation of catalyst

The following mixture compositions was used for the synthesis of MCM-56 with aniline: deionized water, 50% NaOH solution (Sigma Aldrich), sodium aluminate (Riedel–de Haën, 40–45% Na_2O, 50–56% Al_2O_3), hexamethyleneimine (HMI, 99%, Sigma Aldrich), aniline (AN, > 99%, Sigma Aldrich) and Aerosil (A200, Evonic), with molar ratios Si/Al = 12.5, OH/Si = 0.18, HMI/Si = 0.1, AN/Si = 0.2 and H_2O/Si = 45. The gel was reacted in a Teflon-lined autoclave (200 mL) for 240 h at 143 °C with continuous rotation. The solids were isolated by centrifugation, washed three times with deionized water and dried in air. This product was used in subsequent transformations but for characterization it was calcined at 540 °C for 6 h with 2 °C/min ramp, ion exchanged using 1 M ammonium nitrate solution (3 times for 1 h). The same calcination and ion exchange procedure was performed also for all the other studied materials. This sample was labelled as “parent”.

2.1.1. Exfoliation

The colloid suspensions of MWW monolayers were obtained by two methods (see Scheme 1): A – two-step, resulting in lower alkalinity medium, and B – 1-step in 5% TBAOH. In the first approach (A) 0.5 g of the parent, as-synthesized MCM-56-aniline was stirred with 11% tetrabutylammonium hydroxide solution (TBAOH 40% in H_2O, Sigma-Aldrich) for 2 h. The suspension was centrifuged (2 times for 10 min at 10 000 rpm), the supernatant was decanted and the precipitate containing all of the zeolite was stirred with 20 mL of deionized water for 1.5 h. The obtained translucent solution was separated from the solid by centrifugation at 10 000 rpm for 20 min. The supernatant was decanted and precipitated using CTMACl (25% wt. in H_2O, Sigma-Aldrich). The solid was centrifuged out, washed with deionized water (20 mL), dried in air at RT, calcined and ion exchanged. This material was labelled as "A".

In the second approach (B) 0.5 g of the parent, as-synthesized MCM-56-aniline was stirred with a 5% TBAOH solution for 2 h. The slurry was centrifuged and the solution of MWW monolayers was decanted and used for the reaction with the 25% solution of CTMACl (volume ratio 1:2) resulting in immediate precipitation of a white solid. This solid was separated by centrifugation, washed with deionized water (20 mL) and dried in air at RT. The series of material based on this preparation was identified with the letter "B".

2.1.2. Pillaring

The obtained MWW-surfactant composites were pillared by reaction with TEOS in two ways:

1) excess amount of TEOS (1:100 w/w),
2) 1:5 w/w ratio solid to TEOS.

In the 1st method, dried solids were mixed with TEOS (1:100 w/w) and stirred for 1 day or 5 days at room temperature. They were separated on a Büchner funnel, dried at RT, calcined and ion exchanged. The products were labelled as B-pill-1d and B-pill-5d.

In the second method, dried solids were first dispersed in 13 mL of isopropanol (iP) and stirred for 2 h. Then, 2.6 g of TEOS was added and the mixtures were stirred for 1 or 5 days at room temperature. The products were separated on a Büchner funnel, dried at RT, calcined and ion exchanged. The materials obtained using this method were labeled as A-iP/pill-5d, B-iP/pill-1d, and B-iP/pill-5d.

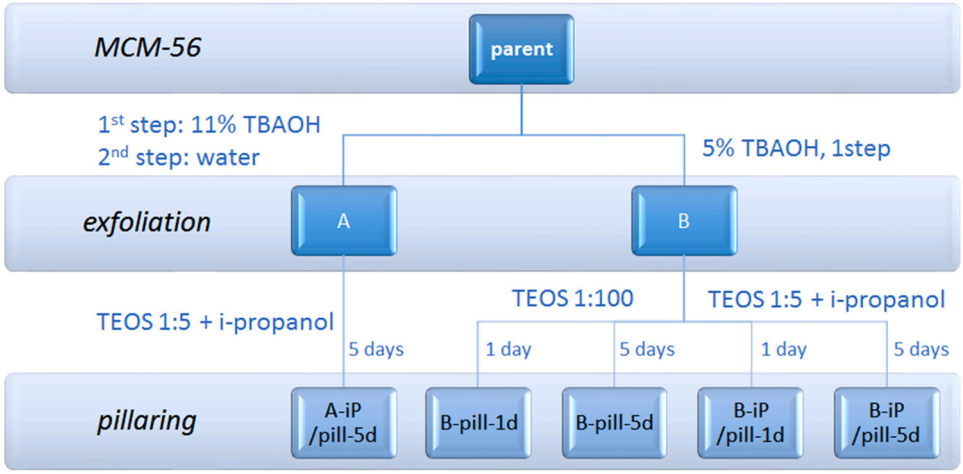

Scheme 1. Modification of the parent MCM-56 zeolite leading to the formation of exfoliated and pillared materials.

2.2. Characterization

2.2.1. Structure

X-ray powder diffraction (XRD) patterns were collected on a Bruker AXS D8 Advance diffractometer equipped with a graphite monochromator, position sensitive detector (Vântec-1) in Bragg-Brentano geometry in the range 1–10° 2θ and Rigaku MiniFlex diffractometer in the ranges 3–30° in reflection mode. Cu K_α radiation (ʎ =0.154 nm) was used in both cases. The XRD patterns were collected with steps of 0.02°.

2.2.2. X-ray fluorescence (XRF)

Relative content of Al and Si was determined in the samples formulated into pellets, 13 mm in diameter, with the use of Energy-Dispersive XRF spectrometer (Thermo Scientific, ARL QUANT'X). The X-rays of 4–50 kV (1 kV step) with the beam size of 1 mm were generated with the Rh anode. The detector used was a 3.5 mm Si(Li) drifted crystal with a Peltier cooling (ca. −90 °C). For quantitative analysis, calibration with a series of metallic standards and UniQuant software (Version 3, Thermo Fisher) were used.

2.2.3. Porosity

Nitrogen adsorption isotherms were measured using a static volumetric Autosorb IQ apparatus (Quantachrome Instruments) at − 196 °C. All samples were activated under vacuum prior to the measurements for 0.5 h at 80 °C, 0.5 h at 120 °C and 8 h at 350 °C (2 °C/min ramp). Values of the specific surface area were determined using the BET method. Values of the mesopore and external surface area as well as of the micro- and mesopore volume were obtained using the t-plot method. Pore size distributions were calculated based on N_2 adsorption data using the NLDFT model provided by ASiQwin (Quantachrome) software for zeolite/silica with cylindrical/spherical pores. The porosity was additionally studied by quasi-equilibrated temperature programmed desorption and adsorption (QE-TPDA) of hexane and nonane. The instrumentation and experimental procedures were described in detail previously [31–33]. Prior to the QE-TPDA measurements a sample (6–7 mg) placed in a quartz tube was activated by heating up to 400 °C (10 °C/min) in the flow of helium (7 cm^3/min), then cooled to room temperature. After activation, the hexane or nonane vapors were added to the helium stream resulting in isothermal sorption at RT. Signal of the thermal conductivity detector, consisting of desorption maxima and adsorption minima, recorded during cyclic heating and cooling of the sample at constant rate, represented a QE-TPDA profile.

2.2.4. Atomic force microscopy (AFM)

Silicon wafers were sonicated in ethanol (96%, p.a. Chempur) for 15 min, dried and placed in UV-ozone cleaner for 30 min. Such cleaned substrates were then placed in the glass vials with polyethylenimine solution (PEI, 600 g/mol, Sigma Aldrich, concentration 1 g/dm^3) in 0.01 M NaCl (p.a. Chempur). PEI deposition was supported by pulse sonication (15 min). After completion, the samples were rinsed with copious amount of deionized water and dried in the stream of argon. Finally, the diluted colloid solution (10-fold) was spin-casted (2 000 rpm, 120 s) on the PEI modified support.

Atomic Force Microscopy (AFM) images were obtained with a Dimension Icon AFM (Bruker) working in the PeakForce Tapping® (PFT) and QNM® modes. RTESPA-150 (Bruker) probe with a nominal spring constant of 6 N/m was used for all measurements. The thickness of the single layer structures was calculated from depth histograms. The percentage of the single layer structure (image area occupied by single layer structure/total surface area covered with sample) was calculated using bearing analysis. The images were captured in a few different places on the sample (resolution 384 ×384, size 5 ×5 μm for bearing analysis and 1.5 ×1.5 μm for analysis of topography, see Fig. 2).

2.2.5. Scanning Electron Microscopy (SEM)

Scanning electron microscopy (SEM) images were recorded using a Tescan Vega3 LMU instrument with a LaB6 emitter. The samples were coated with gold particles before imaging to reduce charging of the crystals.

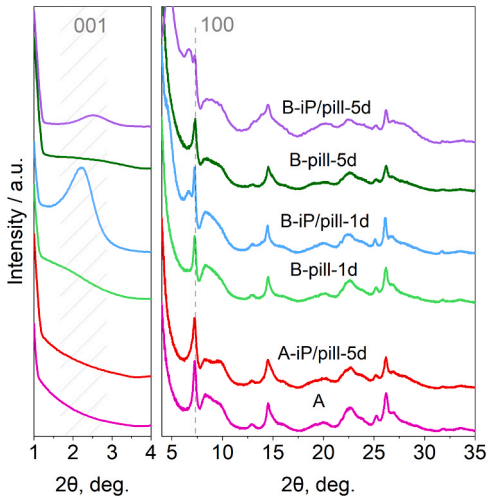

Fig. 1. XRD patterns in the range of 1–4 2θ and 3–35 2θ.

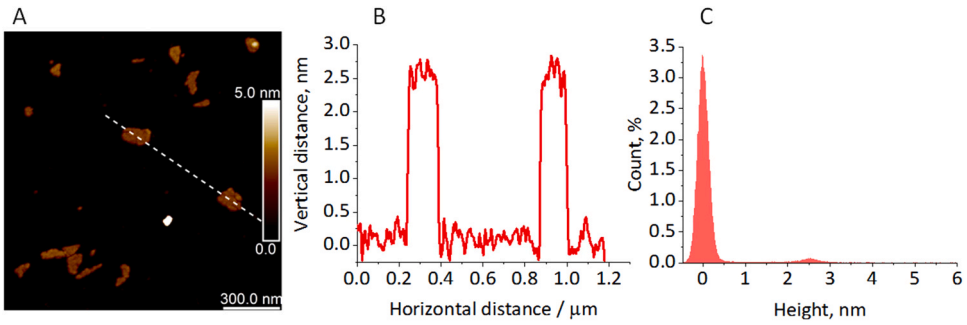

Fig. 2. A) AFM topography image of 10-fold diluted colloidal MCM-56 zeolite suspension deposited on a silicon support modified with polyethyleneimine (PEI) solution, B) cross-section profile captured in the place marked by the gray dotted line and C) depth histogram.

2.2.6. Acidity

The total concentrations of Lewis (LAS) and Brønsted (BAS) acid sites were determined using adsorption of pyridine (Py, anhydrous, 99.8%, Sigma Aldrich), and the concentration of external Brønsted acid sites (BAS_{ext}) by pivalonitrile (trimethylacetonitrile, 98%, Sigma Aldrich) sorption, followed by IR spectroscopy (Tensor 27 from Bruker, MTC detector, spectral resolution 2 cm^{-1}). Zeolites were pressed into wafers and activated in situ at 500 °C for 1 h at high vacuum (10^{-5} mbar) in a home-made quartz cell, equipped with CaF_2 windows. Before adsorption of a probe molecule the system was cooled to the proper adsorption temperature: 170 °C for pyridine and ambient temperature for pivalonitrile. After adsorption of the vapors (at ca. 20 mbar) the gas phase together with weakly adsorbed species were evacuated at the adsorption temperature for 20 min. All spectra presented in this paper are recalculated to the same mass of the pellet (10 mg).

2.3. Catalytic testing

The batch reactor for liquid-phase benzylation of mesitylene with benzyl alcohol consisted of a three-neck round bottom flask equipped with a reflux condenser, with heating in a multi-experiment workstation StarFish (Radleys Discovery Technologies). The reaction temperature was 80 °C. Typically, 22 mL (19 g) of mesitylene was combined with 50 mg of catalyst and 0.1 g of dodecane as an internal standard. The reaction mixture was maintained for 30 min at the required reaction temperature and then 0.2 g of benzyl alcohol was added. This was considered as the beginning of the reaction. Liquid samples (0.4 mL) were withdrawn at regular intervals and analyzed by the gas chromatograph PerkinElmer Clarus 600 GC with the FID detector using a 30 m packed column Elite-1MS.

3. Results and discussion

3.1. Exfoliation of MCM-56 and preparation of pillared materials

As-synthesized MCM-56 was transformed into solutions of monolayers by a soft-chemical exfoliation with tetrabutylammonium solutions in two pathways. The first, denoted low alkalinity or low pH, was carried out in two steps starting with stirring in 11% TBAOH, centrifugation and decantation of the solution that did not contain any zeolite. Water was added to the remaining solid and upon stirring, centrifugation and decantation a translucent liquid containing MWW monolayers was obtained. This solution has pH around 12. The second method using 5% TBAOH is carried out in one step with the layers dispersed in this 'high alkalinity' medium (pH > 13.3, 0.2 M). Both solutions with MWW layers were mixed with 25% solutions of cetyltrimethylammonium chloride (CTMACl) producing analogues of swollen MWW materials with -d-spacing around 5 nm. Pillaring was carried out by contacting the isolated solids with TEOS according to 2 methods: (i) using excess amount of TEOS (1:100 w/w), (ii) using 1:5 w/w ratio solid to TEOS. Additional variations included addition of isopropanol and different times of reactions, 1 and 5 days. The treatments and various pillared samples are summarized in Scheme 1. Two pure zeolite samples were used for reference, the original MCM-56-aniline (parent) and the surfactant precipitated solid (A) after calcination.

3.2. Product identity and quality by X-ray powder diffraction (XRD)

The XRD patterns shown in Fig. 1 allow reliable identification of MCM-56 and its derivatives as random assemblies of MWW layers. This is based on expected features regarding intra- and inter-layer reflection for the MWW structure, published simulations and numerous experimental patterns [34]. The prominent, relatively narrow peaks in the range to 35°2θ at 7.1, 14.2 (calcined), 25 and 26°2θ, assignable to 100, 200, 220 and 310 Miller indices, confirm the MWW structure and to some extent its quality and estimated amount. The second feature, a broad band in the range 8–10°2θ differentiates disordered layer aggregates from the ordered structures, e.g. MCM-22 and MCM-49, which show two sharp 101 and 102 reflections in this region. This wide "band" between 8° and 10°2θ diagnoses absence of ordering in *c* direction [23,35]. The general profile including positions and shapes of broad unresolved bands is also remarkably consistent, proving MCM-56-like structure and layer disorder. The third group of reflections are the interlayer ones, present or absent, which indicate regular layer separation and spacing, if any. All of the solids obtained after precipitation with CTMACl showed a low angle line at the d-spacing of approximately 5 nm indicating the typical multilamellar structure with expanded interlayer galleries and alternating MWW surfactant bilayers [25,34]. As a result of pillaring with TEOS and calcination, only the samples obtained from high alkalinity solutions (series B) show distinct low angle lines, at 4 nm (B-iP/pill-1d) and 3.5 nm (B-iP/pill-5d). Both of these samples also showed an additional peak below 7°2θ of uncertain origin which may be the 003 reflection. It is often observed in swollen MWW materials with CTMACl at 5.5°2θ consistent with 5 nm d-spacing. In contrast to the samples showing distinct low angle 001 peaks in the XRD, those without such peaks are viewed as partially pillared because they show increased textural properties. The exact structure is hard to determine and may include pillared sections (separated by amorphous silica props) with irregular interlayer distance, delaminated-like with disorganized layer arrangements and mesoporous silica domains. The positive effect of high alkalinity can be rationalized as possibly facilitating TEOS hydrolysis. In general, specific explanations are hard to propose because the mechanism of pillaring is not well understood and the presence of isopropanol (iP) compounds the complexity.

3.3. Confirming unilamellar nature of the MWW nanosheets in solution by AFM

The original first exfoliation of MCM-56 with TBAOH [25] was validated by a series of techniques that proved unambiguously the

predominance of unilamellar, 2.5 nm thick nanosheets with the MWW topology in solution. The present preparation with aniline produced analogous solutions in appearance (translucent) and behavior (flocculation with organics) but nonetheless required confirmation. The unilamellar nature of the MWW layers in solution was corroborated by Atomic Force Microscopy (AFM) of diluted samples. The AFM analysis indicated successful exfoliation to separated monolayers (Fig. 2). The thickness of the prepared monolayers 2.5 ± 0.1 nm was determined from depth histograms (examples presented in Fig. 2C) generated from AFM topography maps acquired in a few places on the sample surface. Sporadic double or multi layers of uncertain origin, e.g. initially present or agglomerated after dispersion were detected, but their total contribution in the sample was estimated to 15% by bearing analysis (conducted for two 5 ×5 μm topography maps), while the rest 85% were monolayers.

3.4. Textural properties

They represent the second crucial characterization, after XRD, of the nature and quality of pillared products. Nitrogen adsorption-desorption isotherms presented in Fig. 3 and BET values in Table 1 show that higher alkalinity of the starting MWW layer solutions resulted in greater porosity of the final pillared products. This correlates with the positive results indicated by the XRDs, which showed distinct 001 peaks for samples pillared in the presence of isopropanol. This effect will be further analyzed after presentation of the acid site concentration data. The isotherms obtained for the pure MWW materials, the parent zeolite and the surfactant precipitated colloid, are characteristic for microporous solids possessing low external surface area and large, most probably interparticle mesopores. The isotherms exhibited by the pillared materials show considerable increase of adsorption in the p/p^0 range of 0.05–0.25 (Table 1). The highest BET surface area values were obtained for the TEOS treated samples with isopropanol (1189 m^2/g for B-iP/pill-1d and 919 m^2/g for B-iP/pill-5d). Both showed distinct 001 lines in the XRD.

Calculations of the external and total surface area were based on the analysis of t-plots for the N_2 adsorption isotherms and require additional comments (Fig. S1). For the parent and A samples, only one linear part in the t-plot may be found, which is consistent with prevailing microporosity of these materials. Based on these t-plots, the values of the micropore volume and external surface area was calculated. In contrast, the t-plots obtained for pillared MCM-56 zeolites exhibit two separate linear segments, disjointed by increase of the adsorbed amount corresponding to the capillary condensation in the mesopores. Hence, for each of these materials the t-plot analysis could be performed for each of the separate parts. It resulted in values of the micropore volume and total surface area as well as values of the total pore volume and the external surface area [36]. The total surface area (S_{total}) combines the external and the mesopore surface area, while the pore volume (V_{pore}) is the sum of the micropore and the mesopore volumes. Detailed explanation of the t-plot calculations are shown in Fig. S1.

The differences in mesoporosity of the studied materials are illustrated in Fig. 4 showing pore size distributions (PSD). The parent zeolite and sample A (surfactant preciptated and calcined) have similar PSDs, showing small contribution of the mesopores. The materials from the B series that were synthesized from the solution of higher alkalinity (5% TBAOH) present similar patterns of mesopore size distributions with intense PSD maxima in the range of 5–7 nm and less intense ones at ca 8 nm. Shorter pillaring times resulted in formation of smaller and more uniform mesopores of about 2.6 nm. The material obtained via 1 day isopropanol-assisted pillaring (B-iP/pill-1d) exhibited the highest mesopore volume and external surface area (0.99 cm^3/g and 1189 m^2/g, respectively).

Pore characterization was also carried out by the QE-TPDA method, using hexane or nonane as probe molecules, and the results were consistent with the nitrogen adsorption results. The QE-TPDA profiles of hexane (Fig. 5) characterize in principle the microporosity of the studied samples, as they were recorded at low relative partial pressure of the adsorptive, away from the saturation conditions. All pillared materials exhibit distinct peaks at about 50 °C, observed just after the start of heating in the QE-TPDA desorption phase. They correspond to the strongest adsorption sites located on the external surface or on the surface of the mesopores. Additional wide maxima, observed in the high temperature range (100–200 °C), should be attributed to desorption from the micropores. Their presence confirms that the structural micropores, characteristic for the MWW layers, were to some extent retained after modification.

The QE-TPDA profiles of nonane are dominated by low temperature maxima resulting from desorption from the surface and mesopores (Fig. 6). Additionally, they all show similar high temperature maxima (150–250 °C) corresponding to nonane desorption from the structural micropores. However, desorption patterns in the low-temperature range (25–100 °C) are more diverse. They exhibit one maximum for A-iP/pill-5d, two maxima for B-pill-1d or even three maxima for the other B series materials, thus reflecting complexity of the mesopore systems formed upon pillaring. The first peaks (counting from the low temperature limit) could be attributed to desorption from the external surface. The second peaks may result from desorption from wide mesopores or from instability of the liquid-like adsorbate meniscus in the pores of ca 4 nm. The third peaks should be assigned to desorption from narrow mesopores or large micropores. The pore size distributions calculated from the desorption parts of the QE-TPDA profiles of nonane are in good

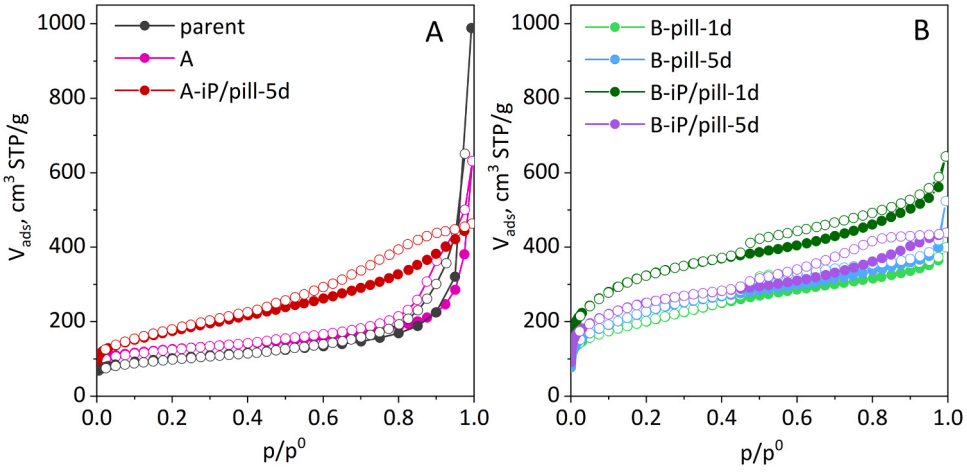

Fig. 3. Nitrogen adsorption-desorption isotherms of studied materials.

Table 1
Porosity data from N_2 sorption, acid site concentration data from pyridine (BAS, LAS) and pivalonitrile (BAS_{ext}) adsorption and catalytic turnover frequency (TOF) in Friedel-Crafts alkylation of mesitylene with benzyl alcohol.

name	exfoliation	pillaring		Si/Al	XRD	surface area [m^2/g]			pore volume [cm^3/g]			acid sites concentration, [μmol/g]			TOF,·10^{-3} s^{-1}
	TBAOH	TEOS	time, days		001 position	[a]S_{BET}	[a]S_{ext}	[a]S_{total}	[a]V_{meso}	[a]V_{micro}	[b]V_{micro}	BAS	BAS_{ext}	LAS	
parent	–	–	–	10	–	369	159	–	0.47	0.03	0.09	607	231	122	2.13
A	11%	–	–	12	–	464	173	–	0.35	0.09	0.27	965	306	150	1.18
A-iP/pill-5d		1:5 +i-Pr	5	10	–	620	170	518	0.67	0.04	0.12	492	264	188	1.17
B-pill-1d	5%	1:100	1	13	–	709	108	599	0.57	0.05	0.12	435	225	187	2.46
B-pill-5d			5	15	–	817	109	795	0.61	0	0.15	500	255	135	2.37
B-iP/pill-1d		1:5 +i-Pr	1	13	4.0	1189	201	1152	0.99	0.01	0.21	442	305	148	4.61
B-iP/pill-5d			5	13	3.5	919	56	844	0.65	0.03	0.21	421	288	230	3.06

[a] N_2 adsorption: S_{ext}, S_{total} and V_{micro} calculated using the t-plot method, V_{meso} calculated as $V_{total}(p/p_0 = 0.97) - V_{micro}$;
[b] calculated from QE-TPDA profiles of hexane, TOF - turnover frequency (TOF) relative to external Brønsted acid sites only, Si/Al based on XRF.

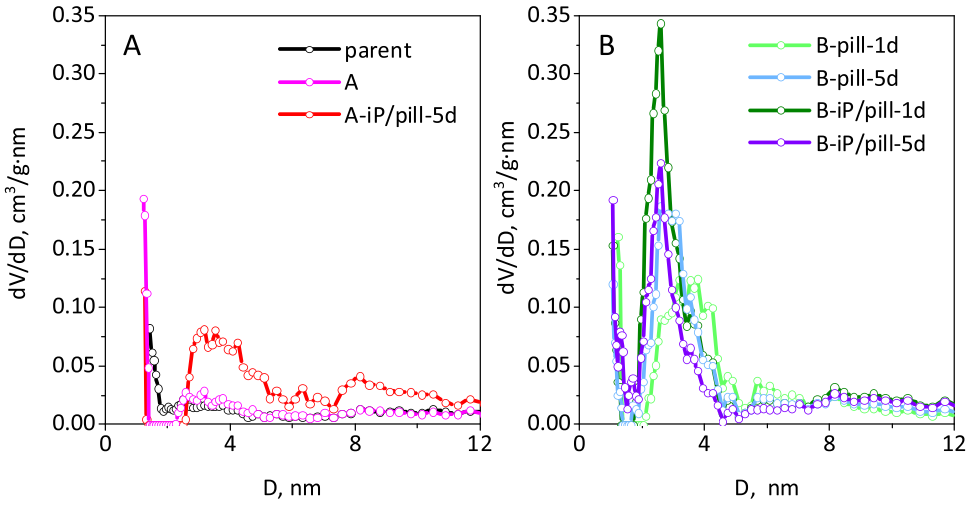

Fig. 4. Pore size distribution calculated using NLDFT method (cylinder/sphere pore model).

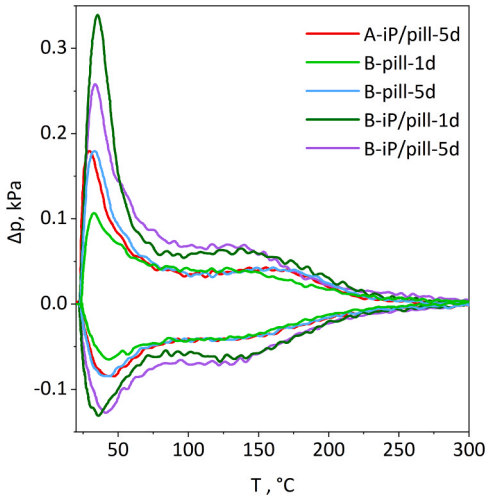

Fig. 5. QE-TPSA profiles for hexane sorption.

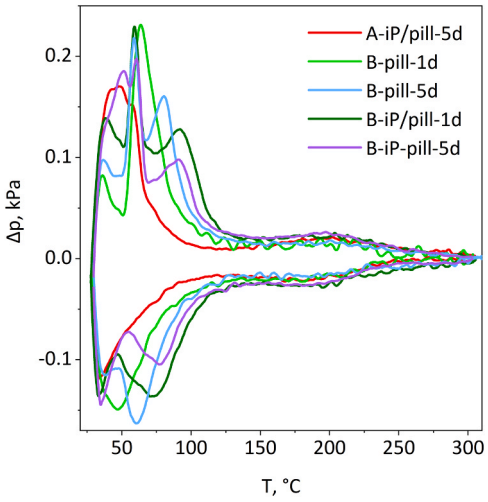

Fig. 6. QE-TPDA profiles for nonane sorption.

agreement with the BJH PSDs based on the desorption isotherms (Figs. S2 and S3). More detailed interpretation of the QE-TPDA profiles of nonane and hexane, observed for modified MWW zeolites may be found in [36] and the references therein.

3.5. Acid site characterization

IR spectra in the region of OH vibrations are presented in Fig. 7. The most intense band, at 3745 cm^{-1}, is characteristic for terminal, isolated silanols. After pillaring the shoulder appears at 3730 cm^{-1}, assigned to hydrogen-bonded silanols which is due to the presence of amorphous silica [35], forming pillars (Fig. 7 and Fig. S4). This shoulder is the most intense for the samples pillared without isopropyl alcohol (B-pill-1d, B-pill-5d). The most important from the standpoint of determination of Brønsted acid site (BAS) concentration is the IR band of the acidic Si–OH–Al groups, which is located at 3622 cm^{-1}, practically the same for all pillared samples. BAS accessibility towards bulky molecules was determined by pivalonitrile sorption. Pivalonitrile cannot diffuse through 10-membered rings of MWW zeolites and therefore allow determination of the concentration of acid sites located at the external surfaces, in the mesopores, and the pore mouths (spectra are presented in Fig. S5). The BAS_{ext} concentration increased from 231 to 305 and to 288 μmol/g for samples pillared in the presence of isopropanol for one and five days respectively, so evidently the shorter treatment leads to material with higher BAS_{ext} concentration.

The striking feature of the pillared materials is similarity of total acid site concentration values (Brønsted plus Lewis, equal to 590–650 μmol/g, Fig. S6) irrespective of the treatments and differences in XRDs and textural properties. This is also reflected by almost constant Si/Al obtained by XRF measurement, which indicated increased Si content in comparison to the parent. It suggests that in all cases similar amounts of silica were deposited during the treatments with TEOS. Acid site blockage is ruled out because the FTIR experiments showed absence of free acid hydroxyl groups after pyridine adsorption (i.e. centers unavailable to pyridine molecule). Similar amounts of introduced silica but different XRD and textural properties can be explained by postulating that higher alkalinity stabilizes the original expanded structure of the MWW-CTMA composites during the reaction with TEOS and promotes the formation of interlayer props. The presence of isopropanol is even more beneficial. In contrast, the composites prepared at lower alkalinity are probably less stable and undergo surfactant leaching before they can be stabilized by the introduction of silica precursor between layers. Previously reported MCM-56 pillaring results obtained in our group [29] showed that BAS concentration could be reduced by more than 90% compared to the parent material and still result in only minor effect on the catalytic activity and indicated that isopropanol-assisted method could be beneficial for the pillaring process.

3.6. SEM images

The images presented in Fig. 8 show the parent zeolite to consist of large agglomerates of layers (exceeding 5 μm in size). These plate-like features, clearly visible on the surface of the parent zeolites agglomerates, disappeared upon modification. Additionally, for the modified material A-iP/pill-5d numerous droplet-like nanoparticles could be noticed on the surfaces of the agglomerates. The materials in B series (especially B-iP/pill-1d) were composed of much smaller and irregular particles (below 1 μm).

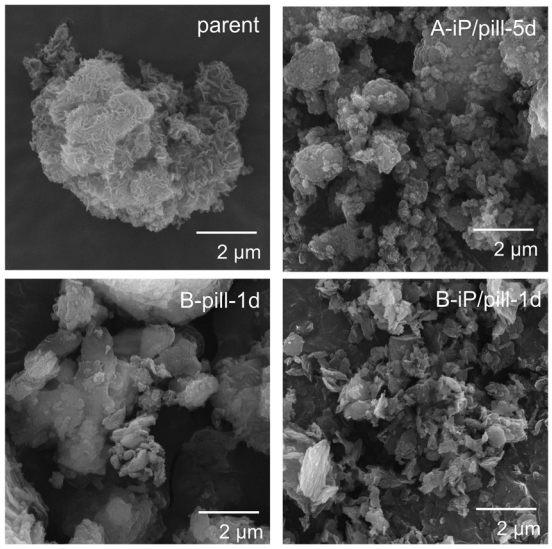

Fig. 8. SEM images of selected materials.

3.7. Catalytic testing

Catalytic activity of the prepared materials was evaluated in a model Friedel-Crafts alkylation of mesitylene with benzyl alcohol, which occurs mainly on external surfaces in the case of MWW materials [14]. The kinetic curves representing time-conversion profiles, shown in Fig. 9, indicate comparable activity of the pure MWW layers – the parent zeolite and the sample A. The pillared material obtained via the low alkalinity route (series A) is less active. The high alkalinity route (series B) affords pillared products that are almost as active as pure MWW layers despite roughly 50% content of inactive silica as pillars. Remarkably, the material with the highest BET shows faster conversion than the starting material and represents, at least nominally, a definite uplift. Its initial slope of the kinetic curve was almost twice that for the parent zeolite, indicating considerable enhancement of the catalytic activity. The observed general trend is that given similar acid site

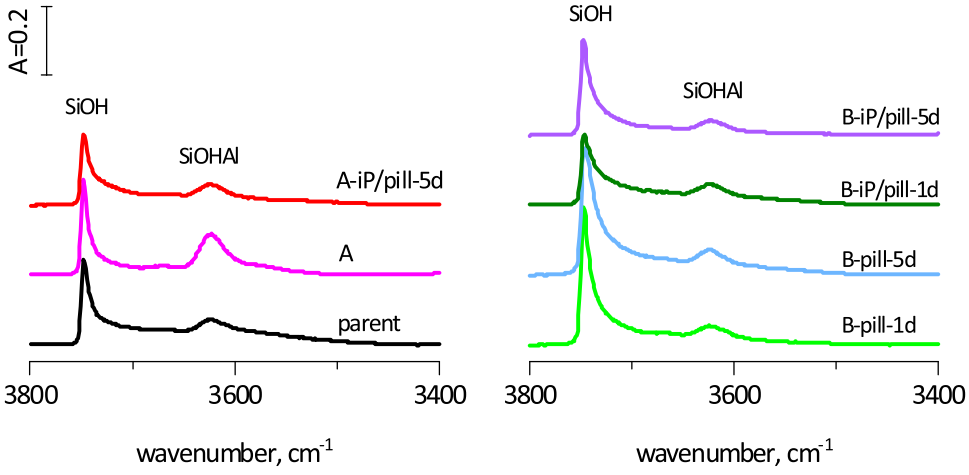

Fig. 7. IR spectra in the OH vbration region for zeolites under study.

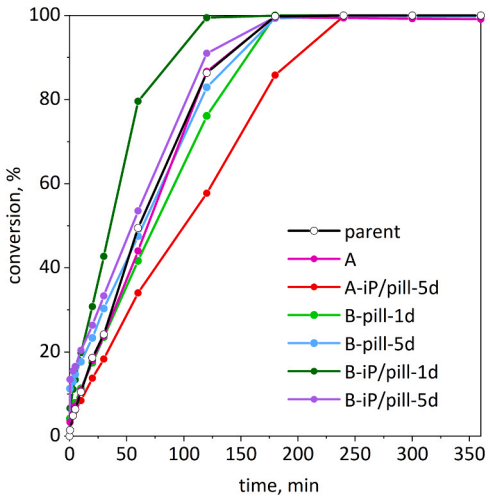

Fig. 9. Conversion of benzyl alcohol in Friedel-Crafts reaction.

concentrations the activity is influenced by the porosity characteristics.

Catalytic activity of the studied material is additionally represented by the relationship between TOF values and the external BAS concentration (Fig. 10). The acid sites of the parent material are more active than the ones present in exfoliated and then recovered sample A and even its pillared version. Pillared materials of the B series, exfoliated at higher pH and having enhanced accessibility of the acid sites, show almost similar values of TOF, except B-iP/pill-1d. This material is the only one to have acid centers of higher activity than the parent material. Addition of isopropanol is much more important in the case of the pillaring process that is carried out for relatively short time. With prolonged pillaring (5 days), the addition of alcohol had no significant effect on the catalytic activity of the resultant material, even if the concentration of the external Brønsted acid sites (BAS_{ext}) increased significantly. The XRD results shows that the materials from the B series are more ordered (presence of the 001 peak), which is obviously positively affecting catalytic performance.

4. Conclusions

The MWW zeolite form MCM-56 was synthesized in the presence of aniline as a structure-promoting agent and proved to represent the second formulation able to produce MWW monolayers solution by exfoliation with TBAOH. These solutions were used to produce pillared MWW materials via precipitation with the cationic surfactant CTMA and treatment with TEOS. Two exfoliation pathways were investigated: lower alkalinity route in two-steps, starting with initial reaction in 11% TBAOH and then after solid separation by centrifugation and dispersion in water and a second route (with higher alkalinity), a single-step exfoliation with 5% TBAOH. Pillaring variable included the amount of TEOS (1:100 or 1:5), duration of treatment (1 or 5 days) and addition of isopropanol. Products were characterized with regard to structure, porosity, acidity and catalytic activity in the alkylation of mesitylene with benzyl alcohol, which probes the micro/mesoporous features. The results clearly indicated that higher alkalinity of the exfoliation is of critical importance. The derivatives are characterized by well-developed surfaces, creating diverse system of pores with the trend toward mesopores. Despite the relatively large amount of silica from TEOS introduction and decreased concentration of acid centers, the activity can exceed that of the pure MCM-56. This suggests that higher alkalinity and inclusion of isopropanol may be the 'best practice' for preparation of pillared MWW materials and maybe other zeolites as well. It has also implications for understanding the conventional pillaring, which usually is done after swelling in basic solution. Apparently, high pH environment is crucial not only for successful swelling but also subsequent

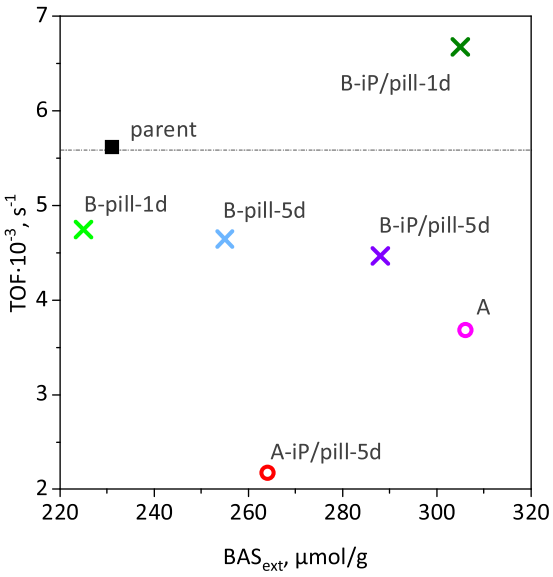

Fig. 10. Dependence of TOF values vs BAS_{ext} concentration.

pillaring, leading to more open and ordered structures with enhanced accessibility of the acid sites and higher catalytic activity.

CRediT authorship contribution statement

Karolina Ogorzały: Investigation, Data Curation, Writing – original draft, Visualization, **Gabriela Jajko**: Investigation, Data Curation, **Karol Wolski**: Investigation, Data Curation, **Szczepan Zapotoczny**: Methodology, Resources, **Martin Kubu**: Investigation, Data Curation, **Wieslaw J. Roth**: Conceptualization, Methodology, Funding acquisition, Supervision, Writing – review & editing, **Barbara Gil**: Methodology, Investigation, Data Curation, Writing – review & editing, Visualization, **Wacław Makowski**: Methodology, Resources, Supervision, Writing – original draft.

Declaration of Competing Interest

The authors declare that they have no known competing financial interests or personal relationships that could have appeared to influence the work reported in this paper.

Acknowledgments

This work was financed with the funds from the National Science Centre Poland, Grant no 2020/37/B/ST5/01258. K.O. has been partly supported by the EU Project POWR.03.02.00-00-I004/16.

Appendix A. Supporting information

Supplementary data associated with this article can be found in the online version at doi:10.1016/j.cattod.2021.10.004.

References

[1] I. Fechete, Y. Wang, J.C. Védrine, The past, present and future of heterogeneous catalysis, Catal. Today 189 (2012) 2–27.
[2] J. Shi, Y.D. Wang, W.M. Yang, Y. Tang, Z.K. Xie, Recent advances of pore system construction in zeolite-catalyzed chemical industry processes, Chem. Soc. Rev. 44 (2015) 8877–8903.
[3] W. Vermeiren, J.P. Gilson, Impact of zeolites on the petroleum and petrochemical industry, Top. Catal. 52 (2009) 1131–1161.
[4] J. Čejka, R.E. Morris, P. Nachtigall, Zeolites in catalysis: properties and applications, The Royal Society of Chemistry, RSC Catal. (2017).
[5] I. Fechete, J.C. Vedrine, Nanoporous materials as new engineered catalysts for the synthesis of green fuels, Molecules 20 (2015) 5638–5666.

[6] M.V. Opanasenko, W.J. Roth, J. Cejka, Two-dimensional zeolites in catalysis: current status and perspectives, Catal. Sci. Technol. 6 (2016) 2467–2484.
[7] W.J. Roth, P. Nachtigall, R.E. Morris, J. Čejka, Two-dimensional zeolites: current status and perspectives, Chem. Rev. 114 (2014) 4807–4837.
[8] W.J. Roth, B. Gil, W. Makowski, B. Marszalek, P. Eliasova, Layer like porous materials with hierarchical structure, Chem. Soc. Rev. 45 (2016) 3400–3438.
[9] E. Schulman, W. Wu, D.X. Liu, Two-dimensional zeolite materials: structural and acidity properties, Materials 13 (2020) 1822.
[10] W.J. Roth, C.T. Kresge, J.C. Vartuli, M.E. Leonowicz, A.S. Fung, S.B. McCullen, MCM-36: the first pillared molecular sieve with zeolite properties, Stud. Surf. Sci. Catal. 94 (1995) 301–308.
[11] A. Corma, V. Fornes, S.B. Pergher, T.L.M. Maesen, J.G. Buglass, Delaminated zeolite precursors as selective acidic catalysts, Nature 396 (1998) 353–356.
[12] U. Díaz, A. Corma, Layered zeolitic materials: an approach to designing versatile functional solids, Dalton Trans. 43 (2014) 10292–10316.
[13] M. Shamzhy, B. Gil, M. Opanasenko, W.J. Roth, J. Čejka, MWW and MFI frameworks as model layered zeolites: structures, transformations, properties, and activity, ACS Catal. 11 (2021) 2366–2396.
[14] D. Liu, X. Zhang, A. Bhan, M. Tsapatsis, Activity and selectivity differences of external Brønsted acid sites of single-unit-cell thick and conventional MFI and MWW zeolites, Microporous Mesoporous Mater. 200 (2014) 287–290.
[15] H.Y. Luo, V.K. Michaelis, S. Hodges, R.G. Griffin, Y. Román-Leshkov, One-pot synthesis of MWW zeolite nanosheets using a rationally designed organic structure-directing agent, Chem. Sci. 6 (2015) 6320–6324.
[16] K. Varoon, X.Y. Zhang, B. Elyassi, D.D. Brewer, M. Gettel, S. Kumar, J.A. Lee, S. Maheshwari, A. Mittal, C.Y. Sung, M. Cococcioni, L.F. Francis, A.V. McCormick, K.A. Mkhoyan, M. Tsapatsis, Dispersible exfoliated zeolite nanosheets and their application as a selective membrane, Science 334 (2011) 72–75.
[17] F.S.O. Ramos, M.K. de Pietre, H.O. Pastore, Lamellar zeolites: an oxymoron? RSC Adv. 3 (2013) 2084–2111.
[18] S. Maheshwari, E. Jordan, S. Kumar, F.S. Bates, R.L. Penn, D.F. Shantz, M. Tsapatsis, Layer structure preservation during swelling, pillaring, and exfoliation of a zeolite precursor, J. Am. Chem. Soc. 130 (2008) 1507–1516.
[19] A. Corma, V. Fornes, J. Martinez-Triguero, S.B. Pergher, Delaminated zeolites: combining the benefits of zeolites and mesoporous materials for catalytic uses, J. Catal. 186 (1999) 57–63.
[20] P. Wu, J.F. Ruan, L.L. Wang, L.L. Wu, Y. Wang, Y.M. Liu, W.B. Fan, M.Y. He, O. Terasaki, T. Tatsumi, Methodology for synthesizing crystalline metallosilicates with expanded pore windows through molecular alkoxysilylation of zeolitic lamellar precursors, J. Am. Chem. Soc. 130 (2008) 8178–8187.
[21] T.F. Degnan Jr., C.M. Smith, C.R. Venkat, Alkylation of aromatics with ethylene and propylene: recent development in commercial processes, Appl. Catal. A Gen. 221 (2001) 283–294.
[22] W.J. Roth, D.L. Dorset, Expanded view of zeolite structures and their variability based on layered nature of 3-D frameworks, Microporous Mesoporous Mater. 142 (2011) 32–36.
[23] W.J. Roth, MCM-22 zeolite family and the delaminated zeolite MCM-56 obtained in one-step synthesis, Stud. Surf. Sci. Catal. 158(A) (2005) 19–26.
[24] G.G. Juttu, R.F. Lobo, Characterization and catalytic properties of MCM-56 and MCM-22 zeolites, Microporous Mesoporous Mater. 40 (2000) 9–23.
[25] W.J. Roth, T. Sasaki, K. Wolski, Y. Song, D.-M. Tang, Y. Ebina, R. Ma, J. Grzybek, K. Kałahurska, B. Gil, M. Mazur, S. Zapotoczny, J. Cejka, Liquid dispersions of zeolite monolayers with high catalytic activity prepared by soft-chemical exfoliation, Sci. Adv. 6 (2020), eaay8163.
[26] E. Xing, Y. Shi, W. Xie, F. Zhang, X. Mu, X. Shu, Perspectives on the multi-functions of aniline: Cases from the temperature-controlled phase transfer hydrothermal synthesis of MWW zeolites, Microporous Mesoporous Mater. 254 (2017) 201–210.
[27] V. Nicolosi, M. Chhowalla, M.G. Kanatzidis, M.S. Strano, J.N. Coleman, Liquid exfoliation of layered materials, Science 340 (2013) 1–18.
[28] M. Osada, T. Sasaki, Nanosheet architectonics: a hierarchically structured assembly for tailored fusion materials, Polym. J. 47 (2015) 89–98.
[29] K. Ogorzały, A. Węgrzyn, A. Korzeniowska, A. Sąwek, A. Kowalczyk, B. Gil, W. J. Roth, W. Makowski, Structure-catalytic properties relationship in Friedel Crafts alkylation reaction for MCM-36-type zeolites obtained by isopropanol-assisted pillaring, Catalysts 11 (2021) 299.
[30] S. Letaïef, M.A. Martín-Luengo, P. Aranda, E. Ruiz-Hitzky, A colloidal route for delamination of layered solids: novel porous-clay nanocomposites, Adv. Funct. Mater. 16 (2006) 401–409.
[31] W. Makowski, Quasi-equilibrated temperature programmed desorption and adsorption: a new method for determination of the isosteric adsorption heat, Thermochim. Acta 454 (2007) 26–32.
[32] W. Makowski, L. Chmielarz, P. Kuśtrowski, Determination of the pore size distribution of mesoporous silicas by means of quasi-equilibrated thermodesorption of n-nonane, Microporous Mesoporous Mater. 120 (2009) 257–262.
[33] W. Makowski, M. Mańko, A. Dudek, K. Mlekodaj, Application of quasi-equilibrated thermodesorption of hexane and cyclohexane for characterization of porosity of zeolites and ordered mesoporous silicas, Adsorption 19 (2013) 537–544.
[34] W.J. Roth, J. Čejka, R. Millini, E. Montanari, B. Gil, M. Kubu, Swelling and interlayer chemistry of layered MWW zeolites MCM-22 and MCM-56 with high Al content, Chem. Mater. 27 (2015) 4620–4629.
[35] V.A. Ostroumova, A.L. Maksimov, MWW-Type Zeolites: MCM-22, MCM-36, MCM-49, and MCM-56 (A Review), Pet. Chem. 59 (2019) 788–801.
[36] W. Makowski, K. Mlekodaj, B. Gil, W.J. Roth, B. Marszałek, M. Kubu, P. Hudec, A. Smieśková, M. Horňáček, Application of quasi-equilibrated thermodesorption of linear and di-branched paraffin molecules for detailed porosity characterization of the mono-layered zeolite MCM-56, in comparison with MCM-22 and ZSM-5, Dalton Trans. 43 (2014) 10574–10583.